SUPPLEMENTARY INFORMATION

Self-assembly of dual-responsive amphiphilic POEGMA-b-P4VP-b-POEGMA triblock copolymers: Effect of temperature, pH, and complexation with Cu^{2+}

Daniela de Morais Zanata and Maria Isabel Felisberti*

Institute of Chemistry, University of Campinas (UNICAMP), P. O. Box 6154, Campinas, SP 13083-970, Brazil

Table of Contents

* Corresponding author: misabel@unicamp.br

1. Structural characterization of POEG$_x$MA$_y$-*b*-P4VP$_z$-*b*-POEG$_x$MA$_y$ copolymers

1.1 ^{1}H NMR spectrum

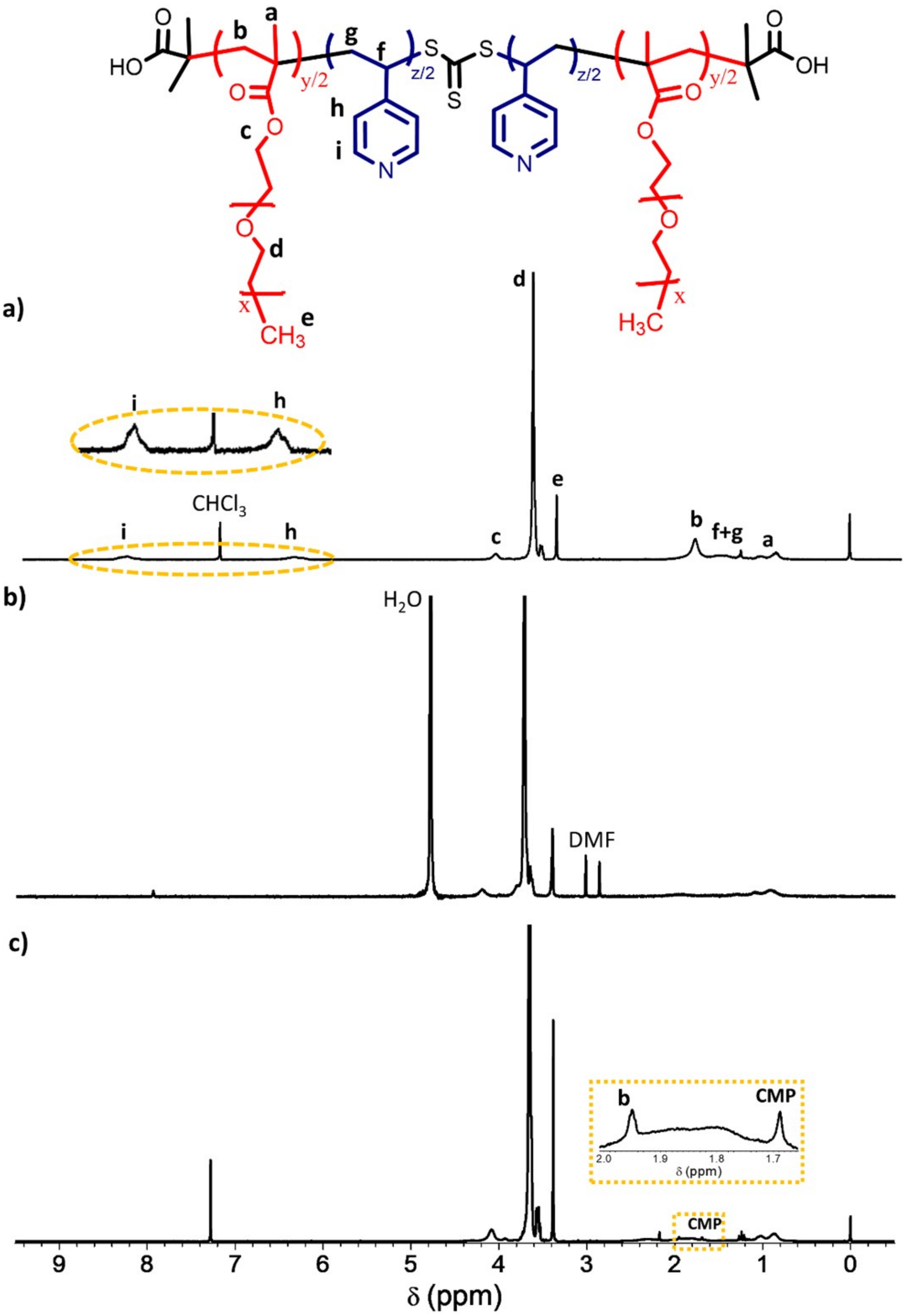

Figure S1. ^{1}H NMR spectra of the POEG$_9$MA$_{26}$-*b*-P4VP$_{56}$-*b*-POEG$_9$MA$_{26}$ copolymer obtained in **a)** CDCl$_3$ and **b)** D_2O as well as the chemical structure of the copolymer with labeled hydrogens. **c)** ^{1}H NMR spectrum of the POEG$_9$MA$_{52}$ obtained in CDCl$_3$. The signals at 7.25 and 4.79 ppm are due to CHCl$_3$ and H_2O residues in the deuterated solvents, respectively.

The degree of polymerization of macro-RAFT $POEG_xMA_y$ (**y**) was calculated using Equation S1 and the ^{1}H NMR spectrum of the purified POEGMA.

$$\mathbf{y} = \frac{H_c}{2} \Big/ \frac{H_{CMP}}{12} \qquad \text{(Equation S1)}$$

where H_c and H_{CMP} are the areas of the signals assigned to the hydrogens H_c of the POEGMA (δ = 4.0 ppm) and of the methyl hydrogens of CMP end chains (δ = 1.69 ppm), respectively.

The number average molar mass (M_n^{RMN}) of the POEGMA block was calculated as the product of **y** and the molar mass of the OEGMA monomers.

The molar (x) and the mass fraction (ω) of POEGMA and P4VP were calculated by using Equations S2a-b and S3a-b, respectively.

$$x_{POEGMA} = \frac{\frac{H_c}{2}}{(\frac{H_c}{2}) + (\frac{H_h}{2})} \qquad \text{(Equation S2a)}$$

$$x_{4VP} = \frac{(\frac{H_h}{2})}{(\frac{H_c}{2}) + (\frac{H_h}{2})} \qquad \text{(Equation S2b)}$$

$$\omega_{POEGMA} = \frac{(\frac{H_c}{2} \times MM_{OEGMA})}{(\frac{H_c}{2} \times MM_{OEGMA}) + (\frac{H_h}{2} \times MM_{4VP})}$$

(Equation S3a)

$$\omega_{4VP} = \frac{(\frac{H_h}{2} \times MM_{4VP})}{(\frac{H_c}{2} \times MM_{OEGMA}) + (\frac{H_h}{2} \times MM_{4VP})}$$

(Equation S3b)

where H_c and H_h are the areas of the signals assigned to the hydrogens H_c of the POEGMA block (δ = 4.0 ppm) and the signals assigned to the aromatic hydrogens H_h of the P4VP block (δ = 6.2–6.6 ppm), respectively. MM_{OEGMA} and MM_{4VP} are the molar masses of the OEGMA and 4VP monomers, respectively.

The degree of polymerization of the P4VP block (**z**) was calculated using Equation S4 and the ^{1}H NMR data of the purified $POEG_xMA_y$-*b*-$P4VP_z$-*b*-$POEG_xMA_y$ copolymers.

$$\mathbf{z} = \frac{x_{4VP} \times y}{x_{POEGMA}}$$

(Equation S4)

The number average molar mass (M_n^{RMN}) of the P4VP block was calculated as the product of **z** and the molar mass of the 4VP monomers.

1.2 GPC chromatograms

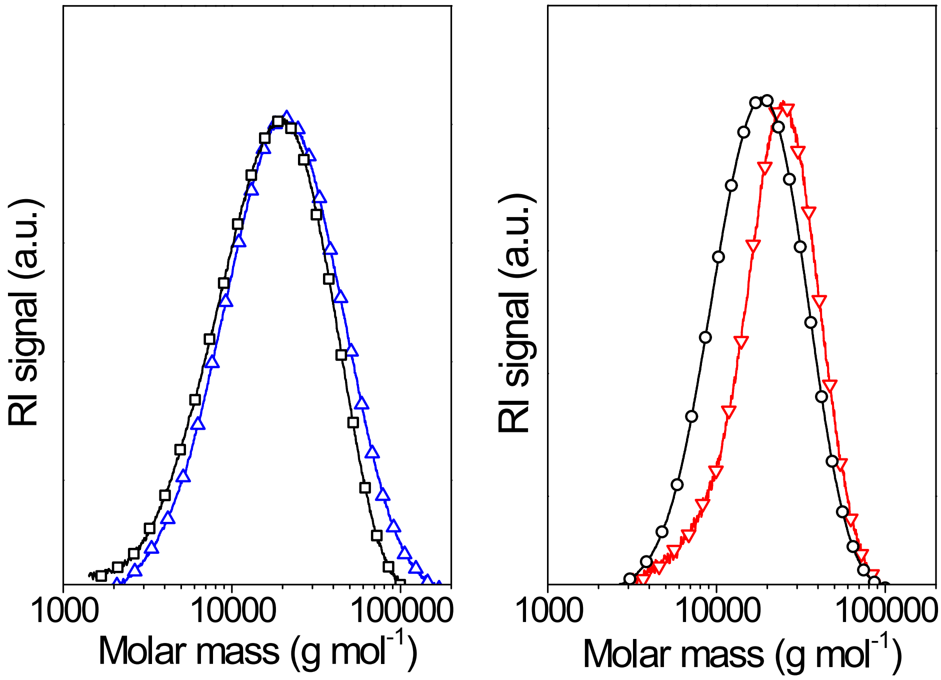

Figure S2. GPC chromatograms of the macro-RAFT agents and their respective copolymers: **a)** (□) $POEG_5MA_{48}$ and (□) $POEG_5MA_{24}$-*b*-$P4VP_{36}$-*b*-$POEG_5MA_{24}$ and **b)** (O)$POEG_9MA_{52}$ and (♦) $POEG_9MA_{26}$-*b*-$P4VP_{56}$-*b*-$POEG_9MA_{26}$. The chromatograms were normalized by the intensity of the peaks.

2. Differential Scanning Calorimetry

Differential scanning calorimetry (DSC) analyses were performed on a TA Instrument MDSC 2910 operating according to the following program: heating from 25 to 120 °C at 10 °C min^{-1}, isotherm at 120 °C for 2 min, cooling from 120 °C to -90 °C at 10 °C min^{-1}, isotherm at -90 °C for 10 min, and heating from -90 °C to 120 °C at 10 °C min^{-1}. DSC scans were normalized to the sample mass.

Figure S3 shows the DSC curve for the $POEG_5MA_{24}$-*b*-$P4VP_{36}$-*b*-$POEG_5MA_{24}$ copolymer. It is noteworthy that the glass transition occurs around -50 °C, which is close to the T_g for the POEGMA macro-RAFT agent. A second glass transition around 155 °C is attributed to the P4VP block[1]. The low ❒C_p associated with this glass transition is due to the lower mass fraction of the P4VP block (22 wt %). The presence of two glass transitions and no first-order transition shows that the copolymer is amorphous and presents microphase separation[2].

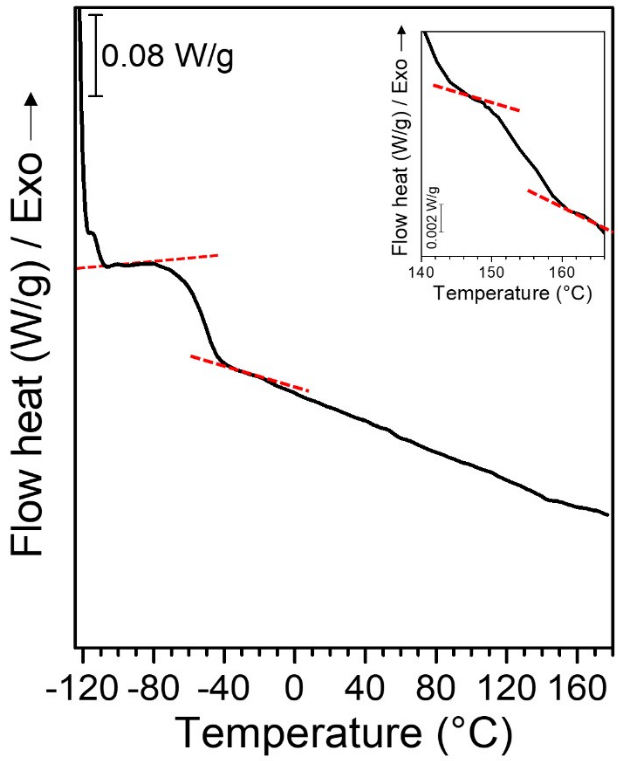

Figure S3. DSC curve of $POEG_5MA_{24}$-*b*-$P4VP_{36}$-*b*-$POEG_5MA_{24}$.

3. Dynamic Light Scattering

3.1 The effect of pH

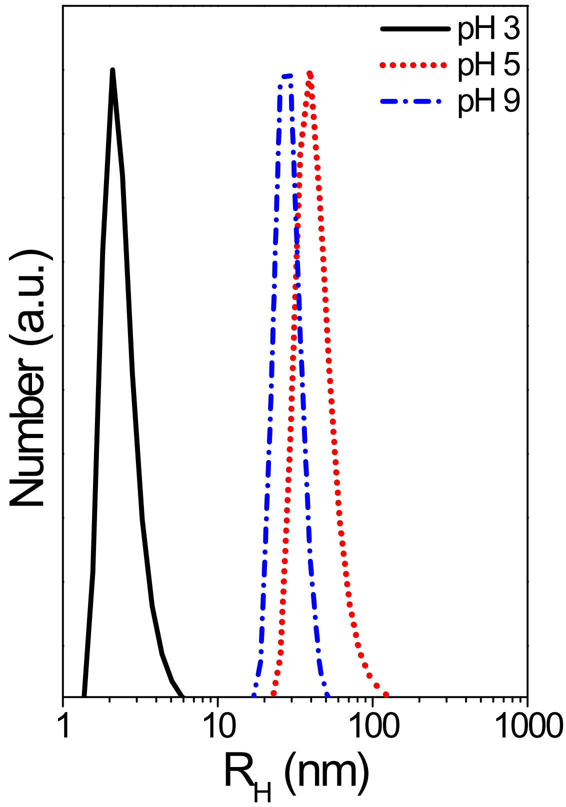

Figure S4. Hydrodynamic radius distribution by number, obtained by DLS, at 25 °C for the $POEG_5MA_{24}$-*b*-$P4VP_{36}$-*b*-$POEG_5MA_{24}$ aqueous solutions, prepared by the water addition method, at (—) pH 3, (• • •) pH 5, and (— • —) pH 9, at 1 mg mL^{-1}.

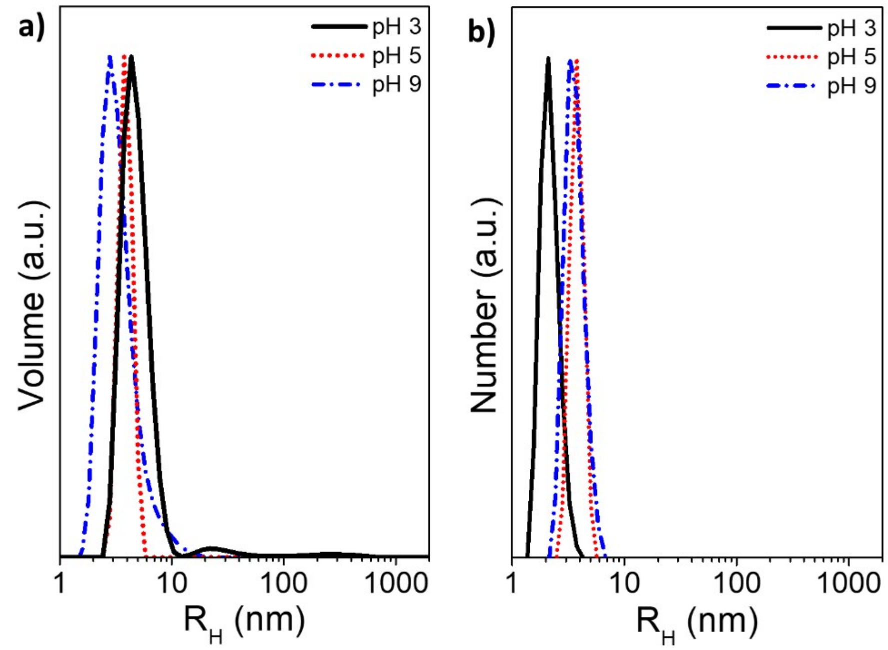

Figure S5. Hydrodynamic radius distribution by **a)** volume and **b)** number, obtained by DLS, at 25 °C for the $POEG_5MA_{24}$-*b*-$P4VP_{36}$-*b*-$POEG_5MA_{24}$ aqueous solutions, prepared by water addition method, at (▬) pH 3, (● ● ●) pH 5, and (▬ ● ▬) pH 9 at 0.5 mg mL^{-1}.

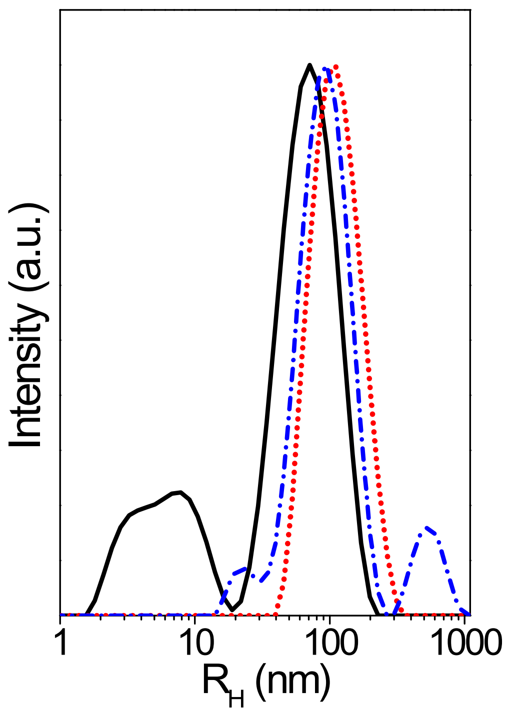

Figure S6. Hydrodynamic radius distribution by intensity, obtained by DLS, at 25 °C for the $POEG_9MA_{26}$-*b*-$P4VP_{56}$-*b*-$POEG_9MA_{26}$ aqueous solutions, prepared by the water addition method, at (▬) pH 3, (● ● ●) pH 5, and (▬ ● ▬) pH 9 at 1.0 mg mL^{-1}.

3.2 The effect of temperature

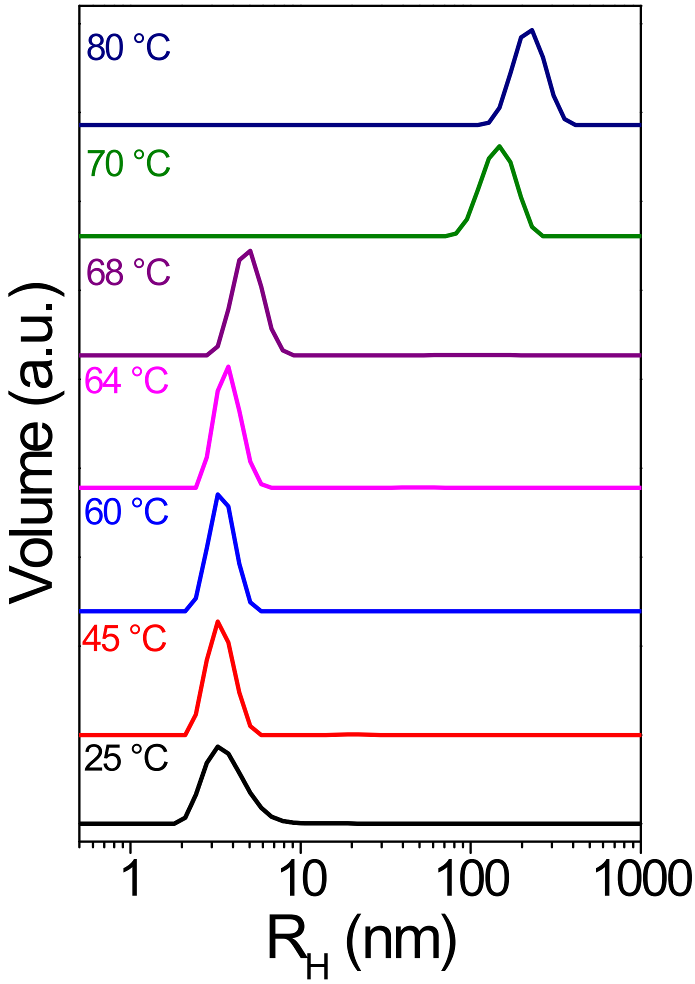

Figure S7. Hydrodynamic radius distribution by volume, obtained by DLS, at different temperatures for the $POEG_5MA_{24}$-*b*-$P4VP_{36}$-*b*-$POEG_5MA_{24}$ aqueous solutions, in the heating step, at pH 3 and 0.25 mg mL^{-1}.

4. Encapsulation of Nile red into $POEG_9MA_{26}$-*b*-$P4VP_{56}$-*b*-$POEG_9MA_{26}$ micelles

(a)

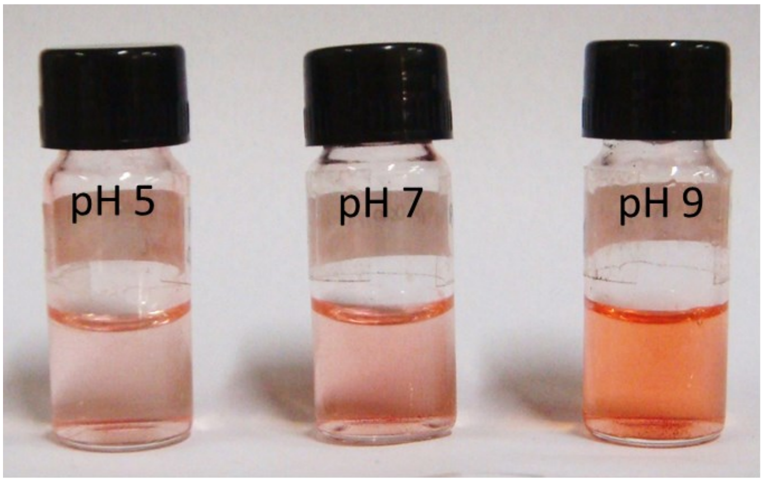

(b)

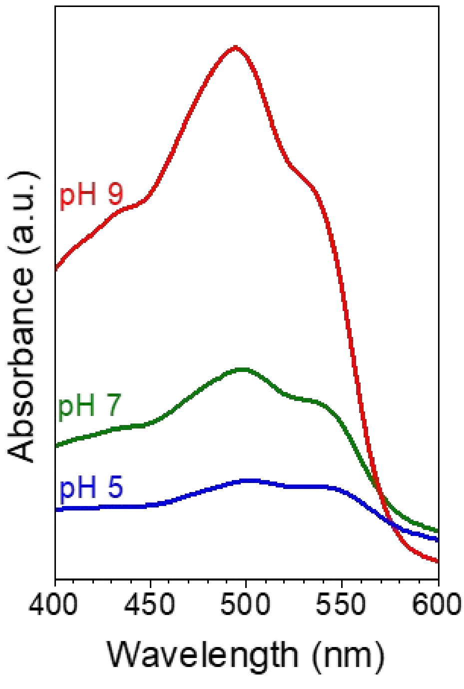

Figure S8. a) Images of the $POEG_9MA_{26}$-*b*-$P4VP_{56}$-*b*-$POEG_9MA_{26}$ copolymer aqueous solutions with encapsulated Nile red at pH 5, pH 7, and pH 9**. b)** UV/Vis spectrum of Nile Red encapsulated micelles of $POEG_9MA_{26}$-*b*-$P4VP_{56}$-*b*-$POEG_9MA_{26}$ aqueous solutions at 0.5 mg mL^{-1}.

5. Complexation of $POEG_5MA_{24}$-*b*-$P4VP_{36}$-*b*-$POEG_5MA_{24}$ with copper

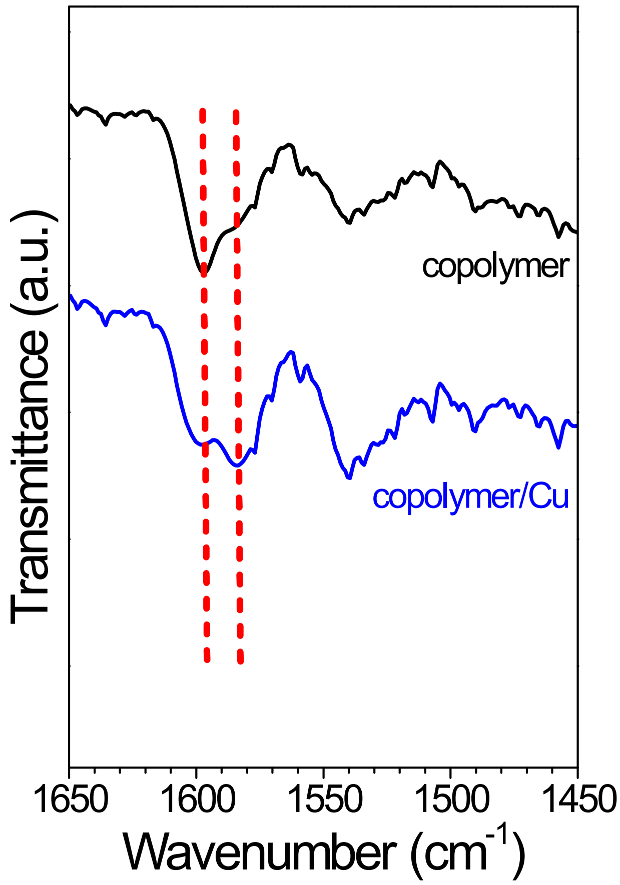

Figure S9. FTIR spectra of the region of the C-N vibrational stretching of the (—) $POEG_5MA_{24}$-*b*-$P4VP_{36}$-*b*-$POEG_5MA_{24}$ copolymer and (—) $POEG_5MA_{24}$-*b*-$P4VP_{36}$-*b*-$POEG_5MA_{24}/Cu^{2+}$.

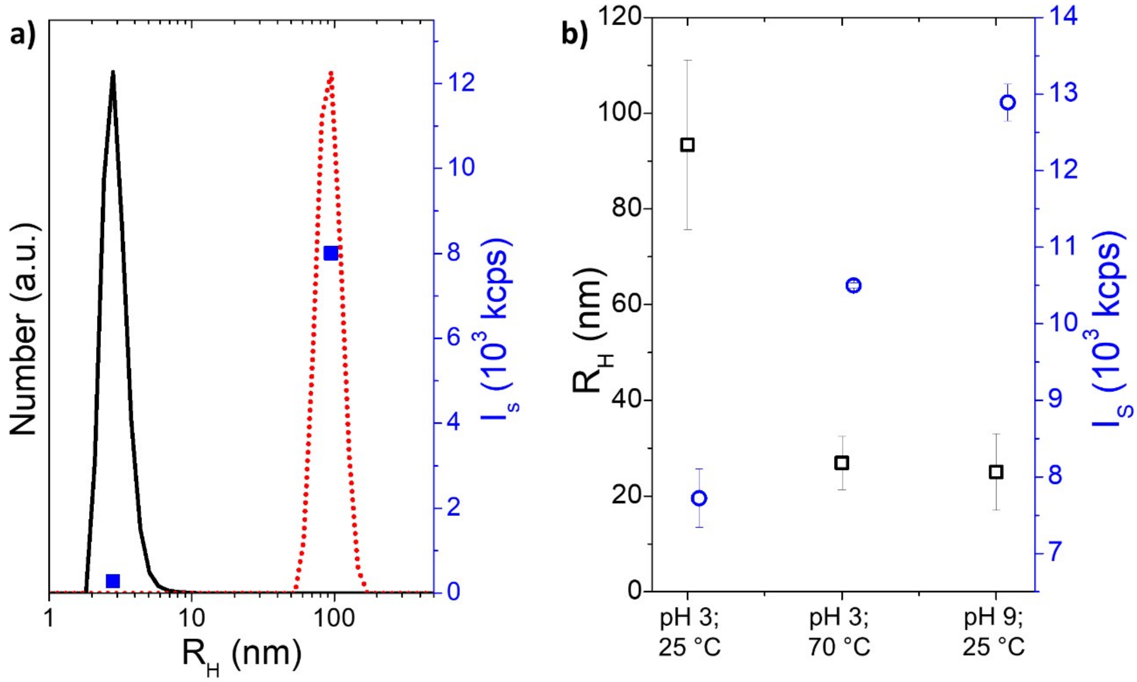

Figure S10. a) Hydrodynamic radius (R_H) distribution by number and (O) derived count rate (I_s), obtained by DLS, at pH 3 and 25 °C for the (—) POEG$_5$MA$_{24}$-*b*-P4VP$_{36}$-*b*-POEG$_5$MA$_{24}$ copolymer and (• • •) POEG$_5$MA$_{24}$-*b*-P4VP$_{36}$-*b*-POEG$_5$MA$_{24}$/Cu^{2+} at 0.5 mg mL^{-1}. The derived count rate is the ratio of the count rate and the attenuation factor. **b)** (□) R_H and (O) I_s for the POEG$_5$MA$_{24}$-*b*-P4VP$_{36}$-*b*-POEG$_5$MA$_{24}$/Cu^{2+}at pH 3 / 25 °C, pH 3 / 70 °C, and pH 9 / 25 °C.

6. References

1 J. Lee, J. Kwak, C. Choi, S. H. Han and J. K. Kim, *Macromolecules*, 2017, **50**, 9373–9379.

2 C. Huang, S. Kuo, J. Chen and F. Chang, *J. Polym. Res.*, 2005, **12**, 449–456.